



ELSEVIER

Available online at [www.sciencedirect.com](http://www.sciencedirect.com)

SCIENCE @ DIRECT®

Deep-Sea Research I ■ (■■■■) ■■■–■■■

DEEP-SEA RESEARCH  
PART I[www.elsevier.com/locate/dsr](http://www.elsevier.com/locate/dsr)

# Davis Strait volume, freshwater and heat fluxes

Jérôme Cuny<sup>a,\*</sup>, Peter B. Rhines<sup>a</sup>, Ron Kwok<sup>b</sup><sup>a</sup>*School of Oceanography, University of Washington, Seattle, Washington, USA*<sup>b</sup>*Jet Propulsion Laboratory, California Institute of Technology, Pasadena, CA, USA*

Received 3 September 2003; received in revised form 29 June 2004; accepted 18 October 2004

## Abstract

Volume, freshwater and heat transport through Davis Strait, the northern boundary of the Labrador Basin, are computed using a mooring array deployed for three consecutive years. The net volume, freshwater and heat transports are  $-2.6 \pm 1.0$  Sv,  $-92 \pm 34$  mSv,  $18 \pm 17 \times 10^{12}$  W. Both southward and northward volume and freshwater transports are maximum in November. The seasonal variability is dictated by the variability in the main water mass transports: Irminger Sea Water, West Greenland shelf water, surface meltwater, and a cold intermediate layer (CIL) originating from Lancaster Sound. The southward freshwater transport seasonal amplitude is dominated by the CIL transport rather than the surface meltwater layer. Sea-ice transport through Davis Strait deduced from remote sensing data is equal to  $528 \text{ km}^3/\text{year}$  which is much smaller than equivalent estimates for Fram Strait. Using these new estimates, we attempt to close the Arctic Ocean volume and freshwater budget.

© 2004 Elsevier Ltd. All rights reserved.

**Keywords:** Davis Strait; Labrador Sea; Baffin Bay; Transports; Freshwater; Sea ice

## 1. Introduction

The Arctic hydrological cycle is a complex combination of land runoff, precipitation, ice freezing–melting and input of salty water from Bering Strait, Fram Strait and Barents Sea shelf. The Arctic Ocean represents only 1% of the world ocean but receives 11% of world river runoff (Shiklomanov et al., 2000). The atmosphere and the ocean play complementary roles as the atmo-

sphere brings moisture to the Arctic and the ocean carries the freshwater southward. Any change in the fresh water flux out of the Arctic affects the nearby ocean convection regions, the Greenland Sea and Labrador Sea. The freshwater route from the Arctic to the Greenland Sea goes through Fram Strait while the route to the Labrador Sea passes through the Canadian Archipelago, into Baffin Bay, and then through Davis Strait (Fig. 1).

Lazier and Wright (1993) estimated that the freshwater flux coming out of Baffin Bay associated with the sea ice melting in that area represents 70% of the freshwater seasonal anomaly

\*Corresponding author.

E-mail address: [jcuny@ocean.washington.edu](mailto:jcuny@ocean.washington.edu) (J. Cuny).

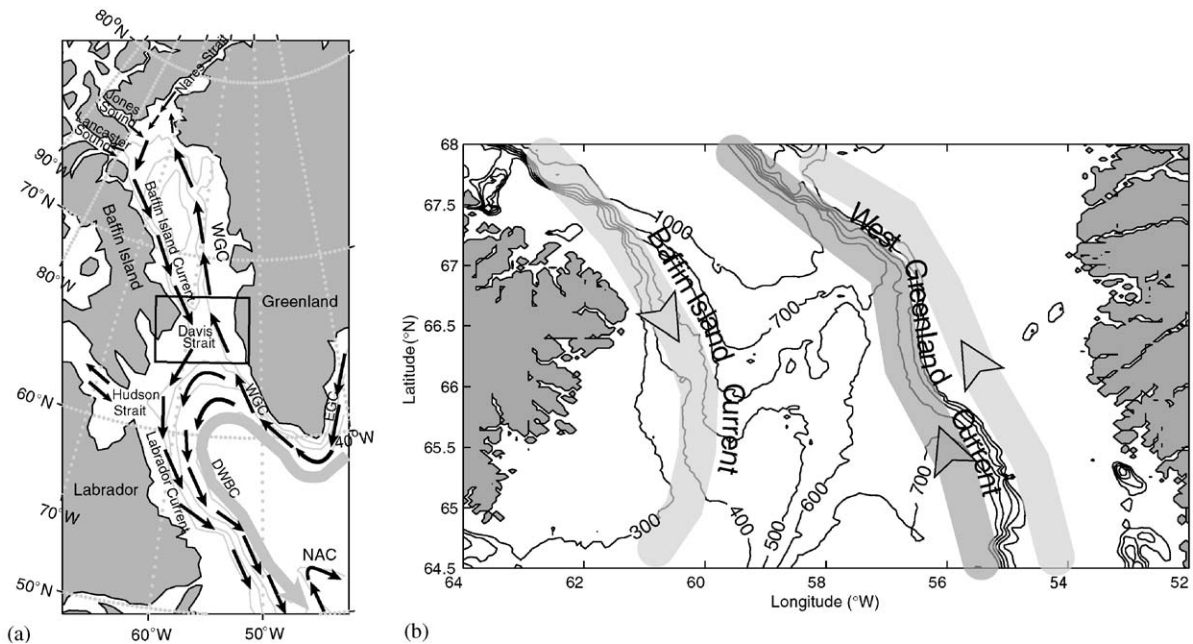


Fig. 1. (a) Circulation diagram for the northwest North Atlantic and Baffin Bay. WGC: West Greenland Current; EGC: East Greenland Current; NAC: North Atlantic Current; DWBC: Deep Western Boundary Current. The rectangle indicates the area shown in (b). (b) Circulation diagram for the Davis Strait region.

downstream on the Labrador shelf. The remaining seasonal freshwater anomaly observed on the Labrador shelf and the interior Labrador Sea are due to the melting of ice drifting with the shelf Labrador Current (Khaliwala et al., 2002). Hudson Bay runoff or sea ice melt is not considered responsible for the Labrador Sea fresh water annual minimum because of the inconsistent timing (Myers et al., 1990).

The thickness and freshness of the cap formed by the freshwater influx atop the Labrador Sea are key components of the convective activity. Goosse et al. (1997) have tested with their model the importance of the fresh water inflow from Davis Strait by opening and closing the Canadian Archipelago passage. They observed a 10% decrease of the overturning circulation when opening the archipelago passage. Wadley and Bigg (2002) suggest from another numerical model run that the decrease could reach 35%. Moreover, Steele et al. (1996) suggest with their model results that in the case of an increased melting of the Arctic Ocean ice, the export of excess fresh water

would be more important through the Canadian Archipelago than through Fram Strait.

Houghton and Visbeck (2002) presented the interannual salinity variations of the freshwater sources for the Labrador Sea, emphasizing the large anomalous events called ‘Great Salinity Anomalies’ (GSA) which were observed at the beginning of the 1970s, 1980s and 1990s. They estimated that the magnitude of the fresh water transport (liquid and sea ice) through Davis Strait was large enough that an anomaly of reasonable amplitude could explain the GSAs in the Labrador Sea. They did not observe a clear decadal fluctuation in the freshwater flowing southward through Davis Strait. However, they found that the salinity had a general downward trend from 1948 till the beginning of the 1990s. On the east side of Davis Strait, the salinity had significant decadal fluctuations clearly related to similar fluctuations in the salinity upstream along the West Greenland coast, but quite different from the signal observed at Cape Farewell. The interaction between the boundary current and the interior

Labrador Sea seems to be the main factor in the salinity fluctuations along the West Greenland coast.

Mean annual volume and fresh water transports in the northwest North Atlantic have been estimated to compute the fresh water budget of the Labrador Sea and to determine the origin of the Middle Atlantic Bight waters (Chapman and Beardsley, 1989; Mertz et al., 1993; Loder et al., 1998). Loder et al. (1998) found that the liquid fresh water input from Davis Strait (120 mSv) represents 60% of the total annual mean fresh water input in the Labrador Sea, thus being the largest source by far. Hudson Strait, the East Greenland Current, precipitation and runoff from Greenland and Labrador are the other main sources. Ingram and Prinsenbergh (1998) estimate that the annual mean sea-ice export through Davis Strait is equivalent to 35 mSv of fresh water, making sea ice a significant factor in the fresh water budget.

The Canadian Archipelago is a complex maze of channels which still need to be monitored accurately over an extended period of time. Davis Strait is a more constrained passage which allows us to measure more easily the exchanges between the Arctic and the North Atlantic subpolar gyre on the western side of Greenland. In this study, we analyze a very complete dataset which covered Davis Strait from September 1987–1990 (Ross, 1992). The dataset includes observations from current meter moorings and hydrographic sections. We also analyzed the sea-ice transport deduced from satellite data through Davis Strait.

The mooring data show that the Davis Strait circulation is mostly a two-way flow with the southward flow covering most of the strait width. We computed the volume, freshwater and heat transport annual cycle from the mooring data. The southward freshwater flow is composed of a surface meltwater layer and a cold intermediate layer (CIL). The amplitude of the seasonal cycle is mostly dictated by the CIL which originates from the Lancaster Sound (Fig. 1). The sea-ice transport through Davis Strait shows significant month to month variability through the winter but no real interannual variability. The heat flux anomaly with respect to 0°C towards the Arctic is mainly defined by the northward

flow of warm Irminger sea water (ISW) and the southward flow of the cold intermediate layer, with sub-zero temperature.

## 2. Data description

### 2.1. Moorings

A set of moorings was placed across Davis Strait between September 1987 and August 1990 (Ross (1992); Fig. 2). The moorings were equipped with Aandera RCM5 current meters. Each instrument was set up to measure at hourly intervals the current velocity, temperature and salinity. Statistics for each mooring are presented in Table 1 and the data return is shown in Table 2. The instruments were located approximately at the same locations during the 3-year period except for one mooring which was displaced from the middle of the ridge during the first year to the eastern flank of the ridge for the two following years. We calibrated the salinity and temperature data by using the available conductivity temperature depth (CTD) casts described below. The numerous gaps in the data prevented us from deducing a 3-year time series at each instrument. An instrument to instrument correlation reveals that instruments from the same mooring are well correlated to each other with a vertical e-folding scale of approximately 400 m in the vertical. However, correlation between instruments from different moorings is very poor suggesting that the mooring array is too sparse to fully capture all the variability in the strait circulation. We assumed that the instruments were close enough from one year to the next that we can average all the data available to obtain one average year of daily data at each instrument location. We considered six mooring locations and three depths (150, 300, 500 m) and called the moorings M1 through M6 starting from the westernmost mooring.

In order to compute meaningful transport estimates, we had to compensate for the lack of data in the top 150 m of the water column. First, we assumed that when the surface above the moorings is covered with ice, the temperature and the salinity are constant from 150 m to the surface.

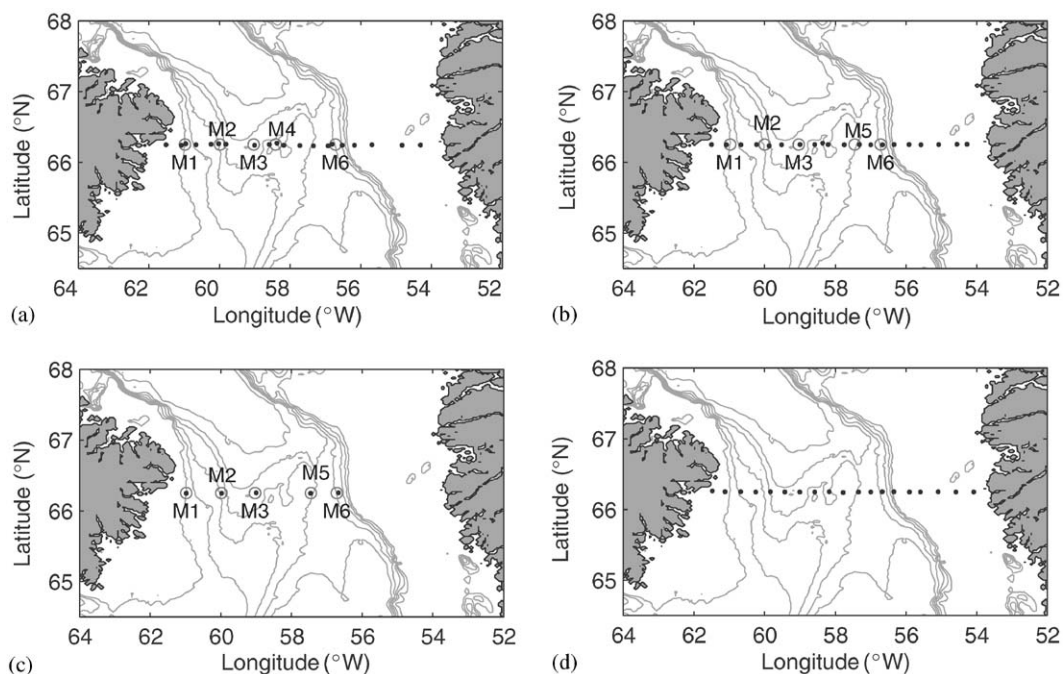


Fig. 2. Mooring and hydrographic station locations in Davis Strait for (a) September 1987, (b) October 1988, (c) September 1989, (d) September 1990. Circles indicate the location of the moorings which were present for the following year. The black dots indicate the hydrographic station location.

Table 1  
Mooring statistics

	Nominal depth in m	( $L$ on, $L$ at) °W, °N	Time period	Zonal vel. mean $\pm$ std in cm/s	Merid. Vel. mean $\pm$ std in cm/s	Speed mean $\pm$ std in cm/s	Temp. mean $\pm$ std in °C	Salinity mean $\pm$ std
M1	157, 153, 142	60.96, 66.26	Sep. 1987	$1 \pm 11.9$	$1.5 \pm 24.8$	$46 \pm 34.9$	$1.5 \pm 0.1$	$33.14 \pm 0.28$
	307, 302, 292		Aug. 1990	$2.2 \pm 7.9$	$4.2 \pm 23.3$	$37.7 \pm 31.3$	$0.9 \pm 0.4$	$33.69 \pm 0.15$
M2	171, 165, 151	59.98, 66.26	Sep. 1987	$1.1 \pm 8.8$	$4.4 \pm 19.9$	$35.1 \pm 24.9$	$1.6 \pm 0.1$	$33.26 \pm 0.28$
	321, 313, 301		Aug. 1990	$0.7 \pm 5.7$	$3 \pm 16.4$	$27.8 \pm 20.8$	$0.3 \pm 0.6$	$33.91 \pm 0.17$
	521, 513, 501			$0.8 \pm 5.8$	$2.1 \pm 13.2$	$23.2 \pm 16.6$	$0.9 \pm 0.1$	$34.39 \pm 0.06$
M3	166, 170, 163	59, 66.25	Sep. 1987	$0.9 \pm 7.8$	$5 \pm 16.9$	$28.5 \pm 20.8$	$1.3 \pm 0.3$	$33.53 \pm 0.15$
	316, 318, 313		Aug. 1990	$0.2 \pm 5.6$	$1.1 \pm 14.8$	$23.1 \pm 16.8$	$0.3 \pm 0.8$	$34.09 \pm 0.12$
	516, 517, 513			$0.2 \pm 4.5$	$0.1 \pm 13.7$	$21.7 \pm 16.5$	$1.3 \pm 0.3$	$34.49 \pm 0.06$
M4	150	58.38, 66.26	Sep. 1987	$2.4 \pm 13.1$	$4.2 \pm 24.6$	$39.9 \pm 29.1$	$0.6 \pm 1.5$	$33.71 \pm 0.2$
	300		Oct. 1988	$0 \pm 7.2$	$0.9 \pm 14$	$20.5 \pm 14.4$	$2.6 \pm 1.3$	$34.41 \pm 0.18$
	500			$3.3 \pm 9.5$	$1 \pm 13.2$	$18.1 \pm 12.7$	$1.7 \pm 0.3$	$34.51 \pm 0.05$
M5	146, 150	57.44, 66.25	Oct. 1988	$2.6 \pm 7.2$	$8 \pm 13$	$27.4 \pm 18.7$	$0.9 \pm 1.8$	$34.13 \pm 0.19$
	295, 300		Aug. 1990	$1.4 \pm 6.6$	$4.7 \pm 12.5$	$20.9 \pm 15.2$	$2.5 \pm 1.4$	$34.46 \pm 0.18$
	495, 500			$1.4 \pm 6.6$	$3.6 \pm 12.3$	$19.7 \pm 14.5$	$2.4 \pm 1$	$34.71 \pm 0.09$
M6	145, 156, 150	56.77, 66.26	Sep. 1987	$2.1 \pm 8.2$	$5.3 \pm 14.3$	$22.3 \pm 18.4$	$2.2 \pm 1.4$	$34.27 \pm 0.15$
	295, 304, 300		Aug. 1990	$1.4 \pm 6.3$	$4.8 \pm 14.3$	$23 \pm 18.2$	$3.8 \pm 0.8$	$34.64 \pm 0.08$
	495, 504, 500			$1 \pm 5.6$	$3.7 \pm 15.1$	$24.7 \pm 18.8$	$3.4 \pm 0.7$	$34.84 \pm 0.09$

Nominal depths are given for each one-year period when the moorings were deployed.

Table 2  
Mooring data return in percentage for each instrument

	Nominal depth in m	( <i>L</i> on, <i>L</i> at) °W, °N	Time period	Velocity data return (%)	Temperature data return (%)	Salinity data return (%)
M1	157, 153, 142	60.96, 66.26	Sep. 1987–Aug. 1990	100, 100, 93	100, 100, 93	100, 100, 7
	307, 302, 292			72, 83, 31	100, 83, 67	98, 83, 66
M2	171, 165, 151	59.98, 66.26	Sep. 1987–Aug. 1990	100, 0, 0	100, 2, 93	100, 0, 93
	321, 313, 301			100, 100, 93	100, 100, 93	100, 100, 93
M3	521, 513, 501	59, 66.25	Sep. 1987–Aug. 1990	14, 100, 93	15, 100, 93	14, 0, 93
	166, 170, 163			100, 0, 67	100, 100, 93	100, 100, 93
M4	316, 318, 313	58.38, 66.26	Sep. 1987–Oct. 1998	91, 100, 1	91, 100, 1	91, 100, 1
	516, 517, 513			100, 93, 93	100, 71, 93	100, 0, 93
M5	150	57.44, 66.25	Oct. 1988–Aug. 1990	100	100	100
	300			100	100	100
	500			100	100	100
M6	146, 150	56.77, 66.26	Sep. 1987–Aug. 1990	100, 94	100, 27	0, 27
	295, 300			100, 94	100, 94	100, 87
	495, 500			76, 94	65, 94	60, 94
M6	145, 156, 150	56.77, 66.26	Sep. 1987–Aug. 1990	91, 100, 93	100, 100, 93	100, 100, 93
	295, 304, 300			63, 100, 93	63, 100, 93	63, 0, 93
	495, 504, 500			2, 100, 0	2, 100, 0	2, 100, 0

Nominal depths are given for each 1-year period when the moorings were deployed.

Our assumption is based on the belief that when sea ice covers the region from December to May, the retreat of the extremely fresh meltwater combined with brine rejection would homogenise the top of the water column. For September, we deduced average temperature and salinity profiles from the September 1987, 1989 and 1990 CTD sections. For October, we used the October 1988 CTD section. For the other ice-free months, we used historical hydrographic data to deduce temperature and salinity profiles at each mooring location. We combined these monthly 0–150 m temperature and salinity CTD profiles with the variations from the shallowest moored instruments to obtain daily *T* and *S* time series for the upper 150 m. Hence, we were able to compute density profiles, and geostrophic velocity with a level of known motion at 150 m, to which we added daily meridional velocity from the top-moored instruments. The estimated velocity uncertainty is from  $10 \text{ cm s}^{-1}$  in the western part of the strait to  $20 \text{ cm s}^{-1}$  in the middle of the strait where the current structure is much more variable. An uncertainty of  $15 \text{ cm s}^{-1}$  over the upper 150 m gives a transport uncertainty of  $0.45 \text{ Sv}$  across

the array. This dataset made of daily salinity, temperature and meridional velocity is used to compute the volume, freshwater and heat transport presented in the following sections.

## 2.2. Hydrographic data

In combination with the mooring programme, hydrographic cruises covering several parts of Baffin Bay including Davis Strait were done during the fall of 1987, 1988 and 1989 (Fig. 2). There was a much larger number of stations covered across Davis Strait in September 1987 and October 1988 than in September 1989 (only one station per mooring). Most of the mooring data stopped before September 1990 when the last cruise was done. We also used data collected by the CCSS Labrador in August–October 1965, which covered a significant area around the Davis Strait.

## 2.3. Sea ice motion data

Several references in the literature have presented methods for extracting ice motion in the

winter (December to May) from SMMR/SSM/I passive microwave data (Agnew et al., 1998; Liu and Cavalieri, 1998; Kwok et al., 1998). Summer ice motion is unreliable because of the confounding effects of surface melt and atmospheric water vapor. The ice area fluxes presented here are produced by the ice tracking procedure described by Kwok et al. (1998). The error on the ice flux estimates includes a spatial and temporal component. The spatial error formula is  $\sigma_F = \sigma_u L / \sqrt{N_S}$  in  $\text{km}^2$ .  $L$  is the length of the line across which the fluxes are computed (345 km for Davis Strait),  $\sigma_u$  is the standard error in motion estimates, and  $N_S$  is the number of independent samples. These numbers give a spatial error of  $1991 \text{ km}^2$  before 1992 ( $\sigma_u = 10 \text{ km}$  and  $N_S = 3$ ) and  $925 \text{ km}^2$  after 1992 ( $\sigma_u = 6 \text{ km}$  and  $N_S = 5$ ). The error over a certain period of time is given by  $\sigma_T = \sigma_F \times \sqrt{N_D}$  in  $\text{km}^2$ .  $N_D$  is the number of observations over the period of time considered. We used monthly values of ice area flux, so the total error on each monthly value of ice area flux is  $7711 \text{ km}^2$  before 1992 ( $N_D = 15$ ) and  $5066 \text{ km}^2$  after 1992 ( $N_D = 30$ ). The results after 1992 are more reliable not only because of the resolution but also because the 37 GHz channel used before rarely allowed flux estimates beyond April, whereas the 85 GHz channel used after 1992 systematically provided data for May.

### 3. Davis Strait circulation

#### 3.1. Mean circulation from hydrographic data

There is a two way flow going through the 600 m deep Davis Strait. Cold and fresh water ( $\theta \sim -1.5^\circ\text{C}$ ,  $32.5 \leq S \leq 33.5$ ) flows south from Baffin Bay with the Baffin Island Current (Figs. 1, 3 and 4). Warm and salty Irminger Sea Water ( $\theta \sim 4^\circ\text{C}$ ,  $S \sim 34.78$ ), remnant of the Gulf Stream water which has travelled around the subpolar gyre, flows north with the West Greenland Current at the bottom on the eastern side of Davis Strait. This current is one of the branches of the system which splits the ISW between the deep Labrador Current, the West Greenland Current Extension and the West Greenland Current (Cuny

et al., 2002). In Baffin Bay, ISW mixes with polar waters particularly in the North Water Polynya region (Melling et al., 2001). On the West Greenland shelf (WGS), fresh and cold water of Arctic origin ( $\theta \sim 2.3^\circ\text{C}$ ,  $32 \leq S \leq 33$ ) which has travelled around Greenland from Fram Strait and Denmark Strait flows northward and forms a density front at the shelf break with the warmer ISW. The densest water crossing the Davis Strait northward is at the bottom of the ISW core with an average potential density of  $27.72\sigma_0$  and some peaks at  $27.78\sigma_0$  recorded at mooring M6.

The large number of hydrographic stations done in September 1987 and October 1988 provides a clear picture of the circulation in the fall (Figs. 3 and 4). We assumed geostrophy with a level of no motion at the bottom. Then at each mooring location, we deduced a barotropic component as the average difference between the 3-day average moored instruments velocity and the CTD geostrophic velocity. We interpolated to obtain the barotropic component at each CTD station location. We must mention that the velocity section was very dependant on the chosen level of no motion, most likely because there is no real level of no motion in the strait. For the WGS, we computed the geostrophic velocity with a level of no motion at the bottom and added the velocity obtained from the shallowest instrument at the easternmost mooring M6 ( $3 \text{ cm s}^{-1}$  for 1987 and  $8 \text{ cm s}^{-1}$  for 1988). This is surely an overestimate as this instrument is close to the core of the shelf break West Greenland Current. However, it was the closest absolute velocity available.

The Baffin Island Current core is located above the 400 m isobath and peaks at the surface at  $15\text{--}20 \text{ cm s}^{-1}$  (Figs. 3d and 4d) with a  $5 \times 10^{-4} \text{ s}^{-1}$  vertical shear in the top 150 m. On the eastern side, the West Greenland Current flows along the shelf break with a maximum speed of  $15 \text{ cm s}^{-1}$  with a  $4 \times 10^{-4} \text{ s}^{-1}$  vertical shear in the top 150 m. We also observed a southward current on the eastern side of the ridge, which we thought at first to be the continuity of the Baffin Island Current travelling around the ridge to reach the eastern flank. This branch can also reach  $20 \text{ cm s}^{-1}$ . Strangely,

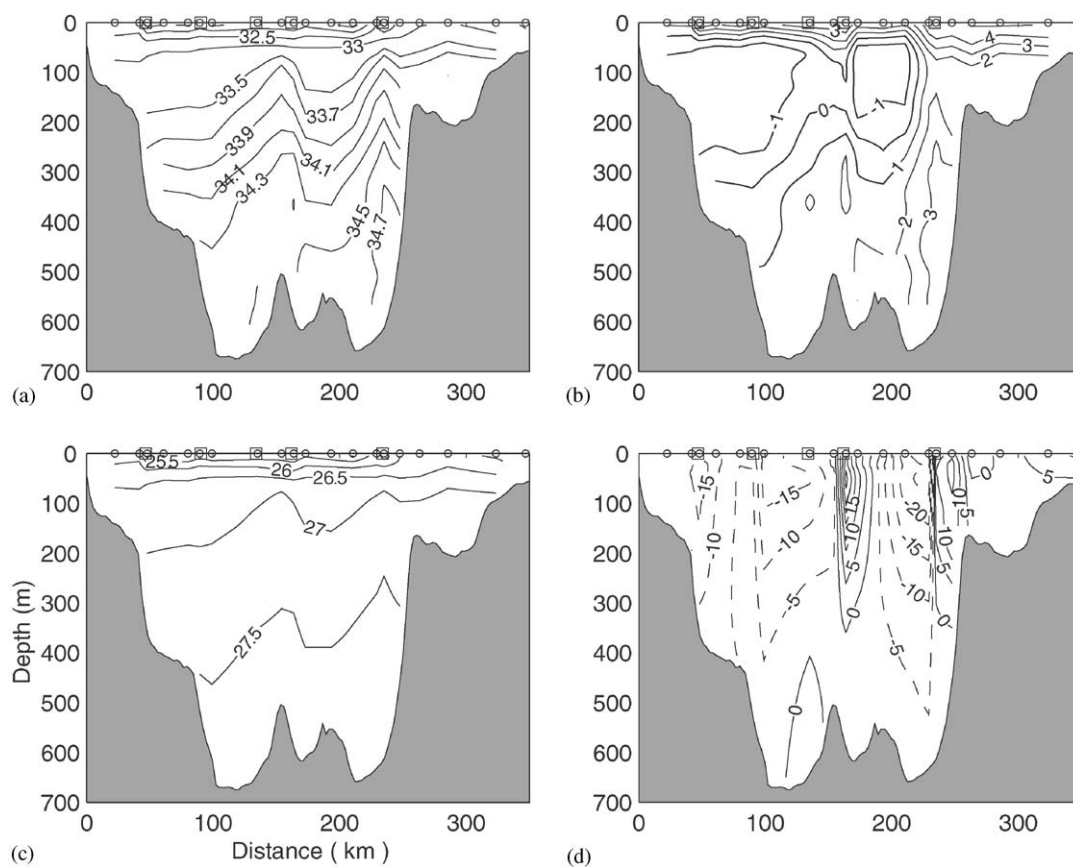


Fig. 3. Salinity (a), Potential temperature ( $^{\circ}\text{C}$ ) (b), Potential density  $\sigma_0$  ( $\text{kg m}^{-3}$ ) (c), and absolute velocity ( $\text{cm s}^{-1}$ ) (d) across Davis Strait in September 1987. The contour intervals are respectively 0.5 from 24 to 33.5 and then 0.2 for 33.7 and beyond for (a),  $1^{\circ}\text{C}$  for (b),  $0.5 \text{ kg m}^{-3}$  for (c), and  $5 \text{ cm s}^{-1}$  for (d). The absolute velocity section is deduced from the CTD section and the mooring data available during the same period of time (see text for detail). The circles indicate the CTD cast locations and the squares indicate the mooring locations available at the time of the CTD section.

we observed a significant northward flow between the two southward branches, evidence of a recirculation west of the ridge, only in the September 1987 section (Fig. 3d). This suggests that the recirculation might not be a permanent feature or that the Baffin Island Current diverges upstream into two branches when the isobaths diverge at around  $67^{\circ}\text{N}$ .

We used the extensive hydrographic survey done in August–October 1965 from  $60^{\circ}\text{N}$  to  $68^{\circ}\text{N}$  to get a better understanding of the 2-D circulation in horizontal space by mapping the dynamic height with respect to a reference depth of 250 m (Fig. 5). There are recirculation regions north and south-

east of the ridge with dynamic height values of 26 dynamic cm. The recirculation north of the ridge, already mentioned earlier was expected due to the southward flow and the ridge shape, but the recirculation south of the ridge was more surprising. It seems that when the West Greenland Current gets closer to the ridge, it gets partially diverted to the south due to the branch of the Baffin Island Current flowing on the eastern flank of the ridge.

On the WGS, speeds can reach  $10 \text{ cm s}^{-1}$ , which agrees well with the speeds measured by two surface drifters that crossed this region in December 1996 and November 1995 (Cuny et al., 2002).

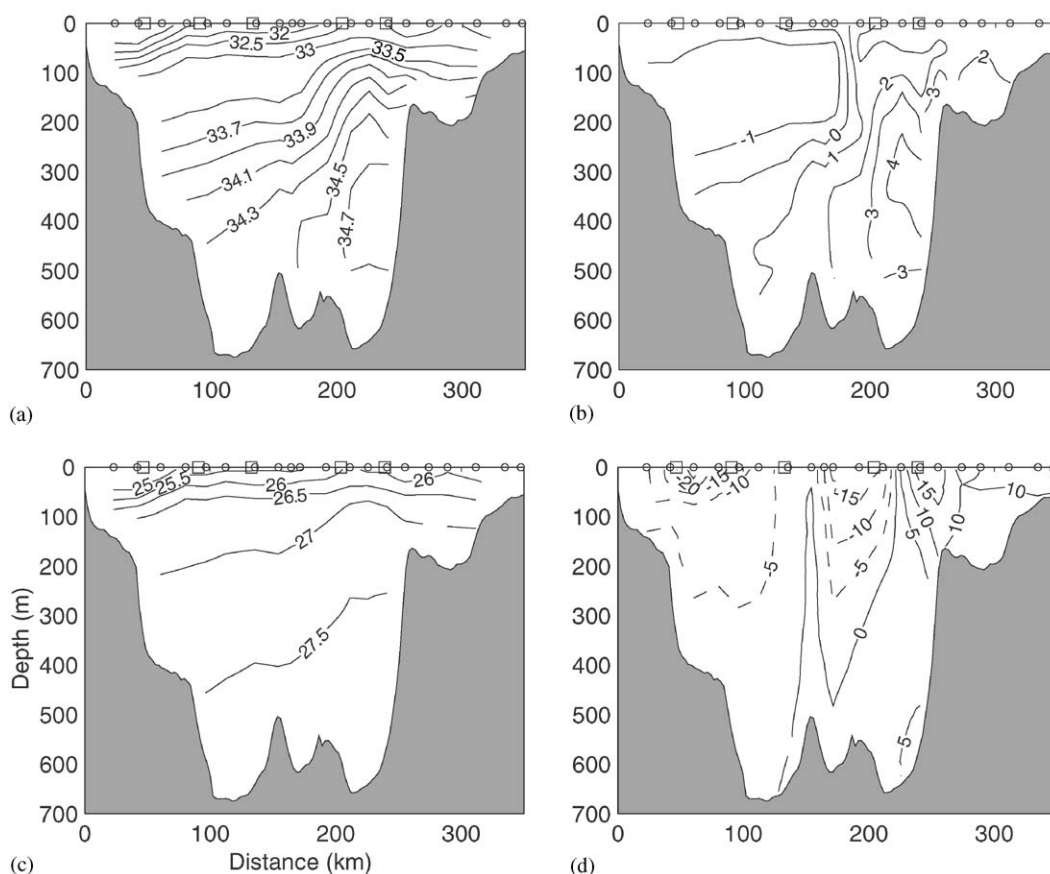


Fig. 4. Same as Fig. 3 but for October 1988.

We notice some evidence of a northward current of low salinity water very close to the coast and separate from the shelf break flow, similar to the East Greenland Coastal Current described by Bacon et al. (2002). The historical hydrographic data on the WGS between 66°N and 67°N (Fig. 6) show that between October and December, when the freshest water is observed, the salinity minimum is found quite close to the Greenland coast, between 30 and 60 km. There seems to be a second minimum closer to the shelf break between 70 and 90 km. There is another salinity minimum very close to the coast around 20 km offshore observed only in summer which could be the continuity of the East Greenland Coastal Current described by Bacon et al. (2002). The waters above the shelf break (120–130 km) show very little seasonal

variability. Considering the error bars, there is a lot of uncertainty in the lateral salinity gradient we just described.

### 3.2. Circulation from the mooring data

We also estimated the mean circulation by averaging the 3 years of the original raw mooring velocity data (Fig. 7). The circulation is essentially a two way flow and matches the description so far. In the western part of the strait, most of the flow converges towards the 600 m isobath as the Baffin Island Current. The fastest flow is always observed at 150 m except at M1, for reasons that we will mention in Section 5. Only M4 seems to have an unusual behaviour with each instrument indicating a different direction. This is most likely due

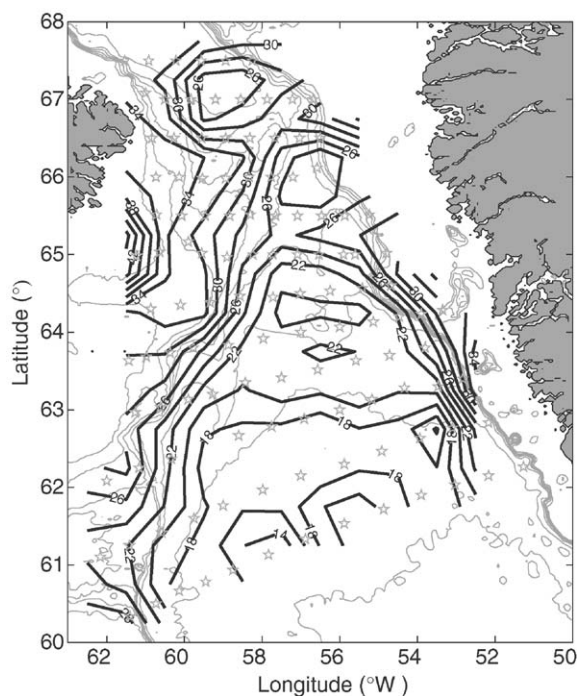


Fig. 5. Dynamic height with respect to 250 m (dynamic cm) from August–October 1965 CSS Labrador hydrographic survey (contour interval 2 cm). Stars indicate the station locations.

to the fact that the mooring was located in a cove of the ridge where local recirculation might dominate.

We computed the mean annual cycle from the three years of the original velocity data (Fig. 8). The northward ISW flow at the West Greenland slope mooring is irregular in strength all year long but is maximum in November with speeds up to  $20 \text{ cm s}^{-1}$  at the surface, when warmer and saltier water is observed (Fig. 9). Interestingly, mooring M5 shows a strong southward flow all year long along the eastern flank of the ridge, with larger values from May to August at 150 and 300 m, and a peak in December at 500 m. All the other instruments show great irregularity in the flow direction and strength. At M1, M2 and M4, the southward flow peaks in October–November at 150 m (Fig. 10). At M1 and M4, the southward flow also peaks in October–November all the way to the bottom. At M2, the peak is observed in August at 300 and 500 m. At M3, the southward

flow is stronger in December–January at all depths.

We also notice an unexpected northward flow at 150 m at M1 from November to February (Fig. 10). Overall, it is very difficult to deduce a clear seasonal cycle of the flow strength at each mooring in the western part of the strait, possibly because of the influence of the convoluted bottom topography.

#### 4. Davis Strait fluxes

##### 4.1. Volume transport

Using the mooring meridional velocity data, we deduced the volume transport annual cycle through Davis Strait. We associate an area to each instrument defined by half the distance with the closest instruments in the vertical and the horizontal direction. In the top 150 m, we consider 75 points, or ‘virtual’ instruments along the profiles described in Section 2 to which we associate an area following the same rule.

The annual mean transports for Davis Strait, excluding the West Greenland shelf, are  $1.2 \pm 0.7 \text{ Sv}$  ( $1 \text{ Sv} = 10^6 \text{ m}^3 \text{ s}^{-1}$ ) northward and  $-4.6 \pm 1.1 \text{ Sv}$  southward (Fig. 11). That last result is larger than previous estimates by Loder et al. (1998) ( $-3.3 \text{ Sv}$ ) and Ross (1992) ( $-3.1 \text{ Sv}$ ) using the same dataset, most likely due to differences in the assumptions for the top 150 m of the water column. They both considered no velocity shear in the top 150 m which makes a significant difference. For instance, a velocity shear of  $2 \text{ cm s}^{-1}$  compared to no shear at all over the top 150 m makes a difference of  $0.27 \text{ Sv}$  over the western part of the strait (180 km wide). Ross (1992) estimated the northward transport at  $0.7 \text{ Sv}$ , which is smaller than our estimate but within our uncertainty range.

The northward transport is minimum in March–April and maximum in November, when the largest velocities are observed and the salinity is close to the annual maximum at M6 (Fig. 9). The southward transport is maximum in November and minimum in March. The error bars represent the standard deviation around the

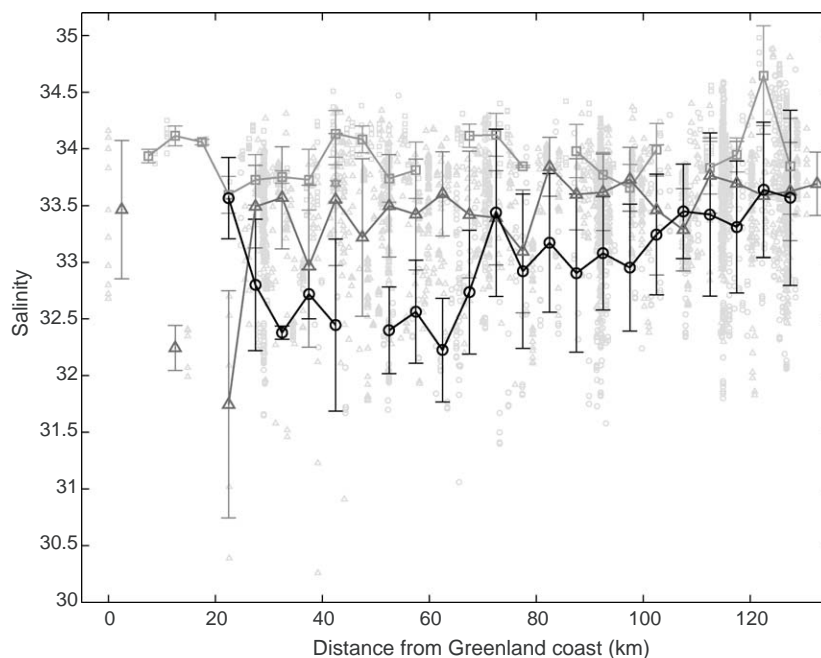


Fig. 6. Salinity across the WGS versus distance from the Greenland coast. We considered the historical data collected between  $66^{\circ}\text{N}$  and  $67^{\circ}\text{N}$  between 1920 and 2000. All the data are shown with the grey symbols. The black lines with symbols show the seasonal mean per 5 km bin. Stars are for winter months (January through March), squares are for spring (April through June), triangles are for summer (July through September), and circles are for fall (October through December). The error bars indicate the standard deviation around each mean. The standard deviation represents an upper bound on the standard error which is defined by  $\text{std}/\sqrt{(N^* - 1)}$ , with  $\text{std}$  the standard deviation and  $N^*$  the effective number of degrees of freedom. The effective number of degrees of freedom is defined as the number of points included in the mean computation, which are statistically independent. We consider a minimum value for  $N^*$  of 2 for each 5 km bin.

monthly mean deduced from the daily transport values. However, we suspect that they underestimate the error as they do not explicitly include the error associated with our assumptions for the top 150 m. Comparisons with the transport estimates from the CTD absolute velocity section presented earlier should provide more realistic uncertainty estimates (Table 3, Fig. 11). The average uncertainty on the mooring estimate is 20% for the northward transport and 40% for the southward transport. The uncertainty for the northward transport seems surprisingly small considering that the northward flow is captured by only one mooring. For the northward transport, the average uncertainty in the top 150 m is twice as big as for the transport below 150 m. For the southward transport, the average uncertainty in the top 150 m is two thirds of the uncertainty

below 150 m. This is expected as the southward transport dominates the section and the top 150 m mooring estimate is dependant on the fall CTD profiles. The CTD transport estimates also reveal that on average 55% of the southward transport and 34% of the northward transport are contained in the top 150 m.

It is interesting to use the CTD data also to look at the transport distribution with respect to temperature and salinity (Fig. 12a, d). We compute the net transport for three main water masses defined by different regions on the  $\theta - S$  diagram: ISW ( $S \geq 34.5$ ), CIL ( $\theta \leq -1^{\circ}\text{C}$  and  $S < 34.5$ ) and the rest of the diagram which includes the surface waters, the WGS and the bottom waters on the western part of the strait ( $S < 34.5$  and  $\theta > -1^{\circ}\text{C}$ ). The bottom waters on the western part of the strait have only a marginal effect on

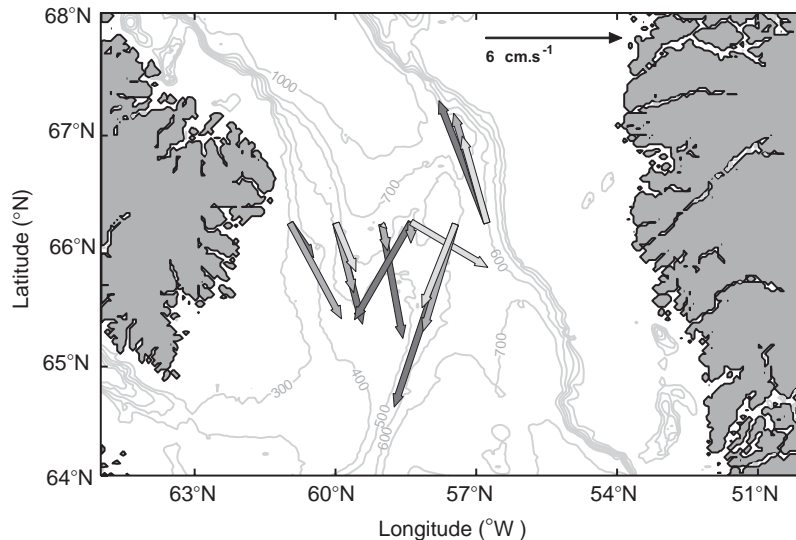


Fig. 7. Three-year mean velocity from the original mooring data ( $\text{cm s}^{-1}$ ). The dark, medium and light grey arrows are respectively for the instruments at 150, 300, and 500 m.

this net transport because of the very weak velocities. Most of the southward transport is associated with cold and fresh water while the northward transport is associated with warmer and saltier waters. We observed slight differences between the 1987 and 1988 results. The largest southward transport is more confined in the range  $33 \leq S \leq 33.5$  with  $\theta$  close to  $-1.8^\circ\text{C}$  in October 1988 compared to September 1987. In both years, there is a significant southward transport of warm and salty water where we expected only northward transport. It is even more marked in September 1987 than October 1988 when the Baffin Island current branch on the eastern side of the ridge entrains a significant amount of ISW southward (Fig. 3d).

The hydrographic estimates used in for the earlier comparisons did not include the WGS component which is not covered at all by the mooring array. Hydrographic transport estimates for the WGS are given in Table 4. This suggests that the mooring array misses a northward transport component possibly as large as 1.6 Sv. We computed an upper limit of the transport over a year by multiplying the velocity given by the top instrument at M6 with the area above

the shelf, assuming that the vertical shear was weak (Figs. 3d and 4d). With that approach September and October transports are, respectively, equal to 0.9 and 1.6 Sv, quite close to the estimates from CTD sections (Table 4). We obtained an annual mean volume transport of  $0.8 \pm 0.8$  Sv on the shelf. Combining the monthly transport time series for the strait and the shelf gives a net transport of  $2.6 \pm 1.0$  Sv southward between Baffin Bay and the Labrador Sea.

## 4.2. Freshwater transport

### 4.2.1. Mean transport

We compute a freshwater transport annual cycle through Davis Strait using the meridional velocity and salinity data described in Section 2. We define the freshwater transport as

$$T_{\text{FW}} = \int \int V \frac{(S_0 - S)}{S_0} dA, \quad (1)$$

with  $V$  being the speed across the section of area  $A$ , and  $S$  the salinity. The reference salinity  $S_0$  is chosen at 34.8. We choose this value for two main reasons. It is the average isohaline between the fresh boundary current water and the offshore

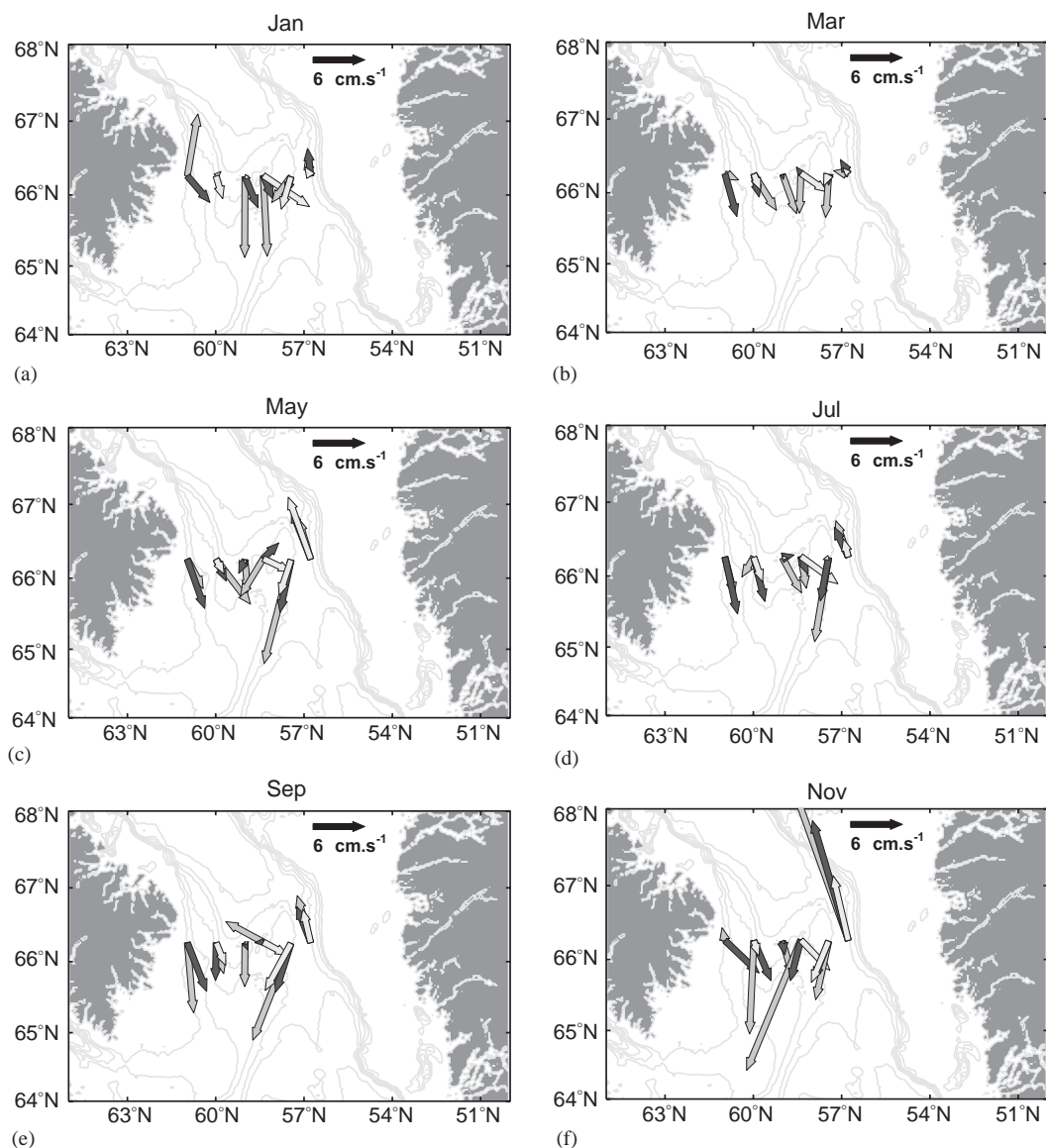


Fig. 8. Mean velocity from the original mooring data for January (a), March (b), May (c), July (d), September (e), and November (f). The dark, medium and light grey arrows are respectively for the instruments at 150, 300, and 500 m.

saltier water in the Labrador Sea on both sides of the basin. It is also considered the mean Arctic Ocean salinity (Aagaard and Carmack, 1989) and the value most used in the literature allowing for appropriate comparisons. A change in the reference salinity of 0.2 can change the freshwater transport by 15% (Loder et al., 1998).

The annual mean freshwater transports excluding WGS are  $22 \pm 17$  mSv ( $1 \text{ mSv} = 10^3 \text{ m}^3 \text{ s}^{-1}$ ) northward, and  $-152 \pm 58$  mSv southward (Fig. 13). The last estimate is close to the 120 mSv given by Loder et al. (1998) for southward transport. The maximum is in October–November for the southward transport which matches with the southward

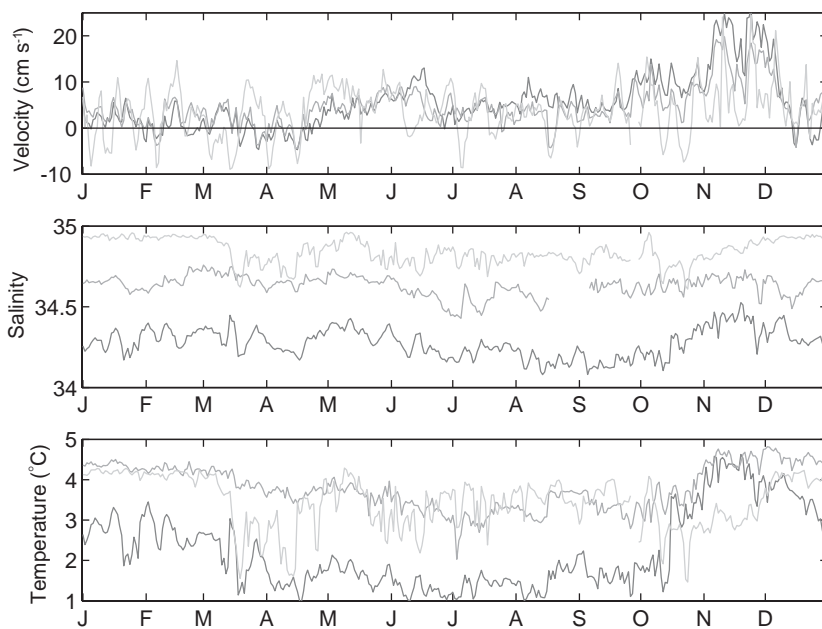


Fig. 9. Daily meridional velocity (top), salinity (middle) and temperature (bottom) at all instruments (150, 300, 500 m) of mooring M6. The dark, medium and light grey lines are respectively for the instruments at 150, 300, and 500 m. Positive velocity means northward.

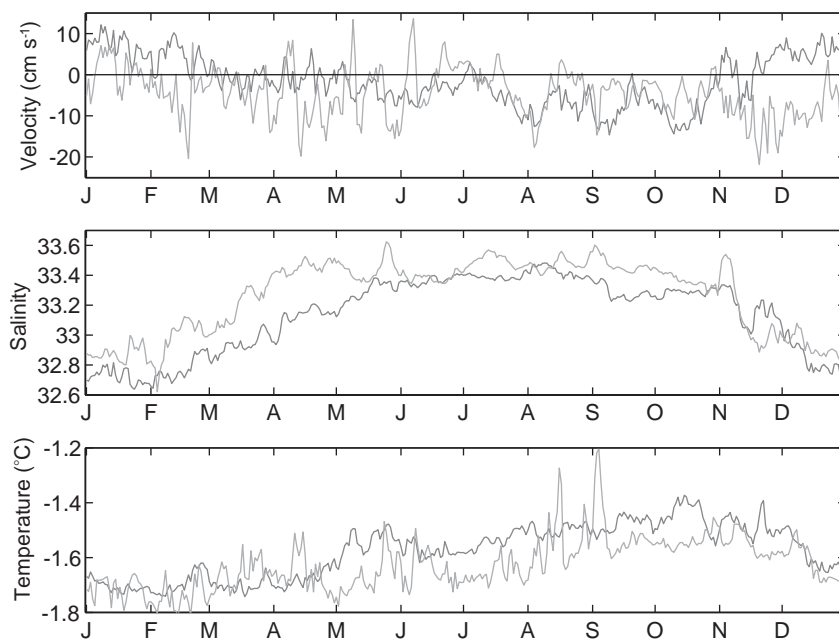


Fig. 10. Daily meridional velocity (top), salinity (middle) and temperature (bottom) at top instruments (150 m) of mooring M1 and M2. The darkest line corresponds to the mooring M1. Positive velocity means northward.

maximum velocity at M2 at 150 m but not with its February salinity minimum (Fig. 10). The maximum northward transport is in November and is associated with high velocities but also with surprisingly salty waters at 150 m (Fig. 9). There is a very good correlation between the freshwater transport and the volume transport (larger than 0.8) suggesting that both the West Greenland Current and the Baffin Island Current are predominantly buoyancy driven.

We compare the mooring estimates to the CTD estimates to get a more realistic range of un-

certainty (Table 3). The average uncertainty is 63% of the mooring estimate for the northward transport and 36% for the southward transport. For the northward freshwater transport, the average uncertainty in the top 150 m is two times larger than for the transport below 150 m. For the southward freshwater transport, the average uncertainty in the top 150 m is one third of the uncertainty below 150 m. The CTD freshwater transport estimates indicate that on average 75% of the southward freshwater transport and 70% of the northward freshwater transport are contained in the top 150 m.

In a similar fashion to our earlier estimate of the net volume transport, we estimated the WGS freshwater transport annual cycle to infer the net freshwater transport between Baffin Bay and the Labrador Sea. We used the M6 top instrument velocity combined with historical salinity data. We obtained freshwater transports for September and October, respectively, equal to 44.5 and 65.6 mSv to be compared with the corresponding estimates from the CTD sections (Table 4). The mean annual transport on the shelf is  $38 \pm 45$  mSv. Hence the net freshwater transport between Baffin Bay and the Labrador Sea is  $-92 \pm 34$  mSv southward, WGS included.

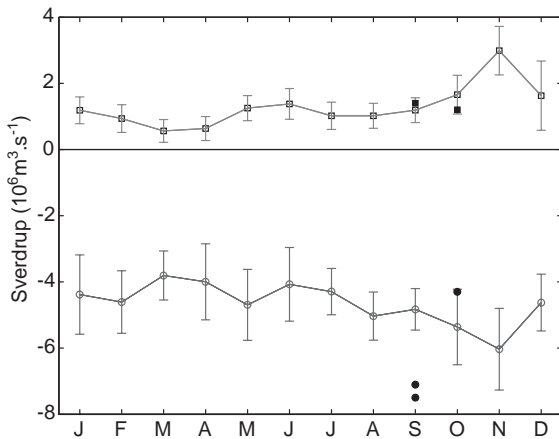


Fig. 11. Monthly mean volume transport ( $Sv = 10^6 \text{ m}^3 \text{ s}^{-1}$ ) through Davis Strait deduced from the 1 year average mooring data, WGS excluded. The negative and positive time series are respectively for the southward and northward volume transport. The error bars are the monthly standard deviation. Solid circles and squares represent, respectively, the southward and northward CTD volume transport estimates (see Table 3).

4.2.2. Seasonal cycle

We tried to explain the southward freshwater seasonal cycle by quantifying the seasonal range of each freshwater source. The seasonal range in southward freshwater transport is 135 mSv which corresponds to a cumulative volume of fresh water

Table 3  
Volume, freshwater and heat transport estimates from the CTD sections for the strait only, WGS excluded

	Absolute transport from CTD section (in $Sv = 10^6 \text{ m}^3/\text{s}$ )		Absolute freshwater transport from CTD section ( $10^3 \text{ m}^3/\text{s}$ )		Absolute heat transport from CTD Section ( $10^{12} \text{ W}$ )	
	Southward	Northward	Southward	Northward	Southward	Northward
Sept. 1987	7.5 (3.8, 3.7)	1.4 (0.9, 0.5)	265.1 (190.6, 74.5)	52 (42.5, 9.5)	25.6 (10.5, 15.1)	28.8 (20.5, 8.3)
Oct. 1988	4.3 (2.8, 1.5)	1.2 (0.3, 0.9)	218.6 (178.3, 40.3)	18.6 (14.5, 4.1)	8 (5.3, 2.7)	27 (11.9, 15.1)
Sept. 1989	7.1 (3.7, 3.4)	1.4 (0.2, 1.2)	298.5 (214.7, 83.8)	12.2 (6.3, 5.9)	16 (8.7, 7.3)	36.7 (11.8, 24.9)

The transport above and below 150 m are given in parenthesis.

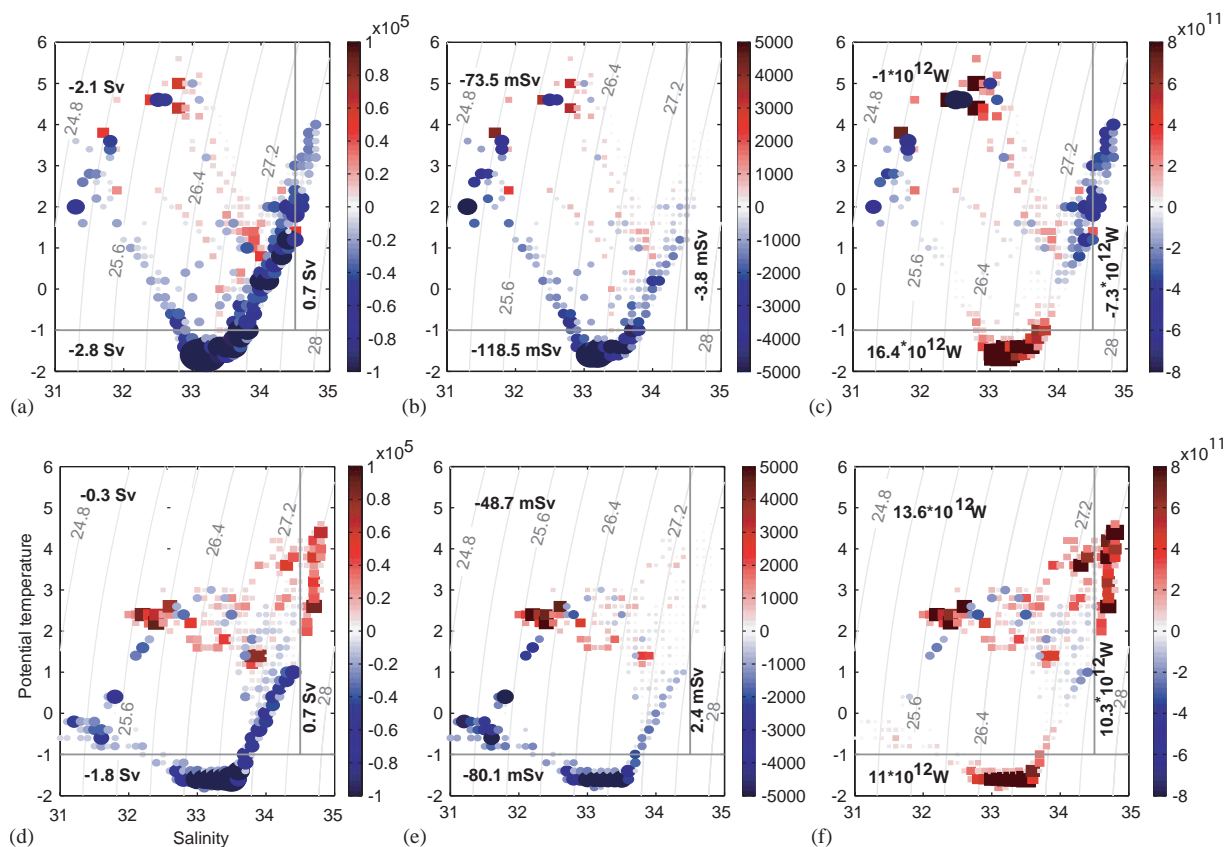


Fig. 12. (a) Volume ( $\text{m}^3 \text{s}^{-1}$ ), (b) freshwater ( $\text{m}^3 \text{s}^{-1}$ ), and (c) heat (W) transport per  $\theta - S$  class from Davis Strait hydrographic section in September 1987, WGS included. (d,e,f) same as for a,b,c but for October 1988. Squares indicate northward transport and circles indicate southward transport. We indicate the transport for three main water masses: ISW ( $S > 34.5$ ), CIL ( $\theta < -1^\circ\text{C}$  and  $S < 34.5$ ) and the surface waters ( $S < 34.5$  and  $\theta > -1^\circ\text{C}$ ).

Table 4  
CTD transport estimates for the WGS

	Geostrophic transport ( $10^6 \text{ m}^3/\text{s}$ )		Absolute transport ( $10^6 \text{ m}^3/\text{s}$ )		Fresh water transport ( $S < 34.8$ ) ( $10^3 \text{ m}^3/\text{s}$ )		Heat transport ( $10^{12} \text{ W}$ )		NAO index
	Southward	Northward	Southward	Northward	Southward	Northward	Southward	Northward	
Sept. 1987	0.1	0.1	0.02	0.4	1.1	18.3	0.4	5.2	-0.75
Oct. 1988	0.03	0.3	0	1.6	0	73.5	0	16	0.72

of  $-12 \times 10^{11} \text{ m}^3$  (Fig. 14a) from May to November. The Baffin Bay sea-ice area annual cycle is presented in Fig. 14b. Assuming an ice thickness of 1 m from mid-March to mid-June, 0.7 m from mid-

June to mid-July, 0.5 m from mid-July to mid-August and 0.3 m from mid-August to mid-September (National Ice center data (<http://www.natice.noaa.gov/eastarct.htm>)), we find that the

volume of fresh water equivalent to the vanishing sea ice is  $-3.9 \times 10^{11} \text{ m}^3$  (see Section 4.3 for formula). The vanishing ice either melted or was advected south out of Baffin Bay. As mentioned in the data presentation, the scatter-

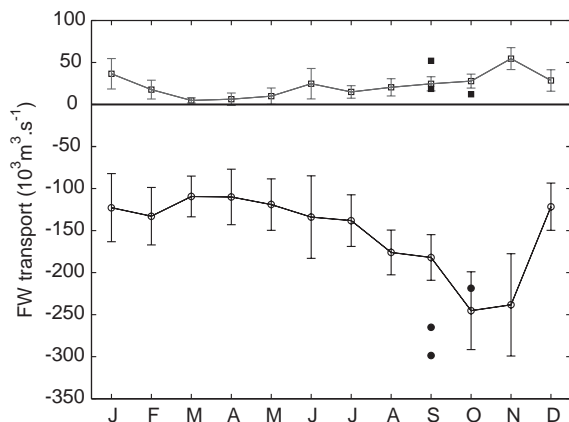


Fig. 13. Monthly mean freshwater transport (mSv,  $10^3 \text{ m}^3 \text{ s}^{-1}$ ) through Davis Strait deduced from the 1 year average mooring data, WGS excluded. The negative and positive time series are respectively for the southward and northward freshwater transport. The error bars are the monthly standard deviation. Solid circles and squares represent, respectively, the southward and northward CTD freshwater transport estimates (see Table 3).

rometer instruments cannot detect ice motion beyond the month of May. We had to rely on the work done by Jordan and Neu (1982), who measured the ice width and speed at Davis Strait from NOAA-5 weather satellite pictures over a year. Using the mean April and May sea ice flux deduced from SSM/I over 1992–2000 and the conditions described by Jordan and Neu (1982) in 1979 for June and July, we find that the volume of fresh water equivalent to the cumulated southward transport of solid sea ice through Davis Strait from April to July is roughly  $-1.3 \times 10^{11} \text{ m}^3$ . We assumed an ice thickness of 1 m in April–May and 0.7 m in June–July. As Baffin Bay is ice free at the end of summer, this means that the remaining  $2.6 \times 10^{11} \text{ m}^3$  corresponds to melted water. In order to infer the amount of meltwater going through Davis Strait, we used results from Tan and Strain (1980), who separated meltwater from meteoric water (precipitation, runoff and glacier melt) using  $\delta^{18}\text{O}$  and salinity. They found that in the western part of the strait the meltwater concentration went from 0 at 35 m to 15% at the surface. We applied this gradient to our daily velocity field and computed the freshwater transport in the top 35 m of the water column assuming a salinity of 5 for the meltwater. The volume of

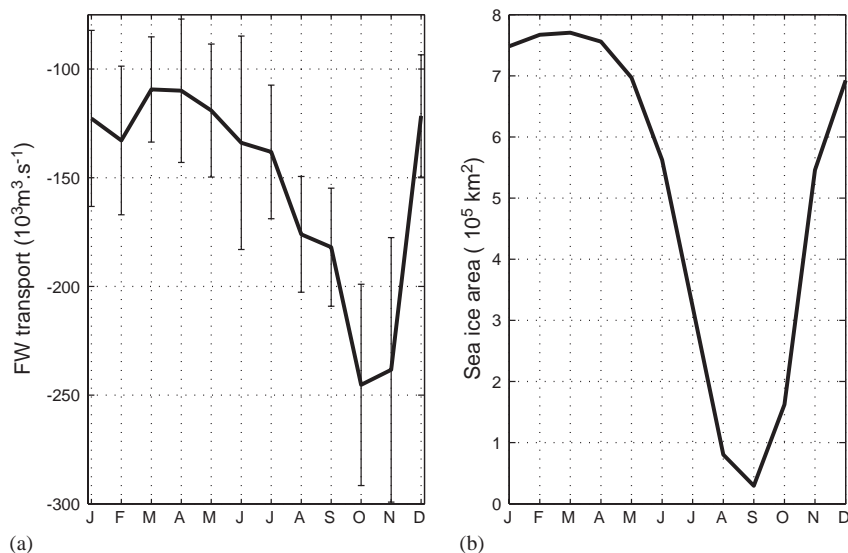


Fig. 14. (a) Southward freshwater transport from the one year average mooring data. The error bars represent the standard deviation around the monthly mean transport values. (b) Baffin Bay sea ice area ( $\text{km}^2$ ) mean annual cycle.

fresh water equivalent to the meltwater going through Davis Strait from May to November is  $-0.8 \times 10^{11} \text{ m}^3$ . This volume is surprisingly small as we expected the melting sea ice in Baffin Bay to have a larger impact on the freshwater transport seasonal cycle. This implies that two thirds of the meltwater from Baffin Bay sea ice recirculates within Baffin Bay and that the meteoric waters (river runoff + precipitation) are a main factor for the seasonal cycle in southward freshwater transport at Davis Strait. The freshwater transport distribution per  $\theta - S$  (Fig. 12b, e) separates the input from two different water masses in the southward transport: one located at the surface with density between  $25$  and  $25.5\sigma_0$  and salinity between  $31.5$  and  $32$ , and the other one located around  $150 \text{ m}$  with density between  $26.5$  and  $27\sigma_0$  and salinity between  $33$  and  $33.5$ . The cumulative transport in the latter class is the largest. If the meltwater estimate is realistic, we deduce that the deeper fresh water class is more important for the seasonal cycle in transport.

Using Baffin Bay hydrographic data, we located the source of this CIL (Figs. 15 and 16). The water observed at Davis Strait in the density range  $26.5-27\sigma_0$  is not a mix of WGS water with waters from the Canadian Archipelago. The western Davis Strait profiles do not lie between the profiles from the eastern Baffin Bay and the profiles from the different straits on the  $\theta - S$  diagram (Fig. 16). It is indeed very close to the profiles from the southern Lancaster Sound suggesting that it is overwhelmingly influenced by Arctic water coming through Parry Channel. Macdonald et al. (1989) suggest that this water mass is a combination of Pacific water and Beaufort shelf water which spilled off the shelf when its salinity increased due to ice formation. This agrees with the high Pacific water concentration observed in the western part of Davis Strait (Jones et al., 2003). Hamilton et al. (2002) reported that a  $170 \text{ m}$  deep instrument in Lancaster Sound recorded a salinity minimum in June–July at  $90^\circ \text{W}$ . Combining the mooring data from different sources (Hamilton

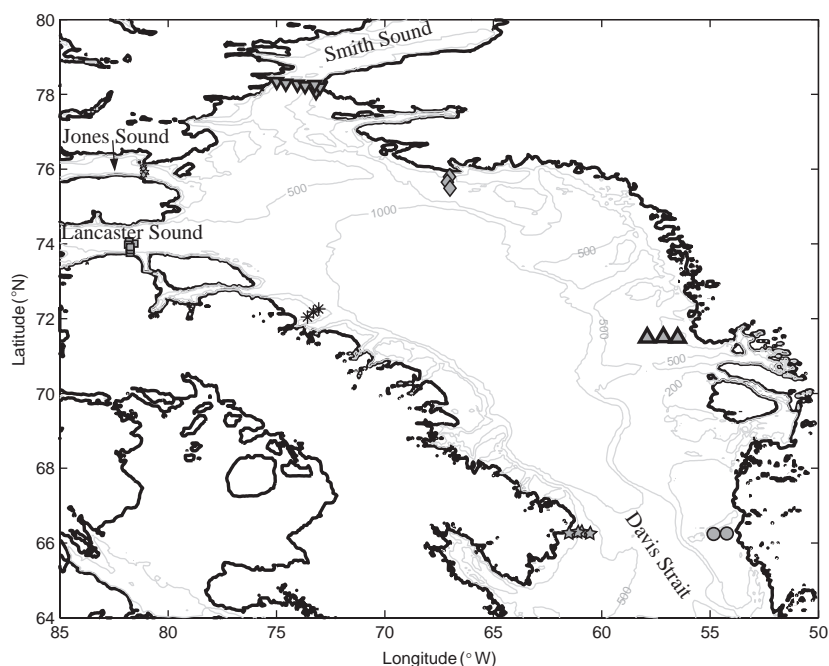


Fig. 15. Locations of the stations used for the evolution of the shelf waters around Baffin Bay shown in Fig. 16. The data were collected at different times: West Greenland shelf  $66^\circ \text{N}$ ,  $71.5^\circ \text{N}$ ,  $76^\circ \text{N}$  (September 1987), Smith Sound (Aug. 1980), Jones Sound (Aug. 1983), Lancaster Sound (Aug. 1983), Baffin Island coast  $72^\circ \text{N}$ ,  $66^\circ \text{N}$  (September 1987). The 200, 500, and 1000 m isobaths are shown.

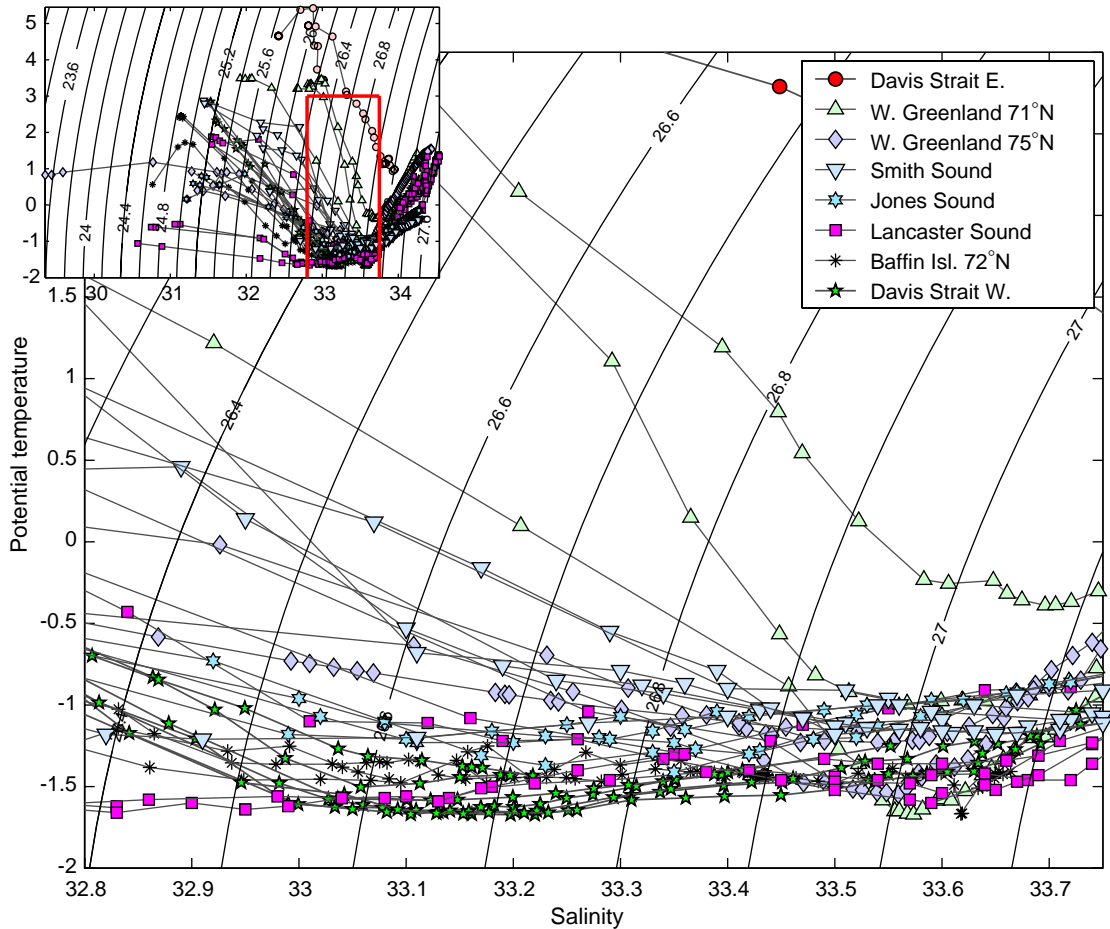


Fig. 16.  $\theta - S$  diagram showing the evolution of the shelves water masses around the Baffin Bay. Each marker used correspond to the marker showing the station location in Fig. 15. We focus on the CIL with density between  $26.5$  and  $27\sigma_0$ .

et al., 2002; Lemon and Fissel, 1982; Ross, 1990a, b), we estimated a transit time of 180 days from Lancaster Sound to Davis Strait. This would explain the salinity minimum observed in December–February in the western part of the strait (Fig. 10).

We used the mooring array to deduce the lateral distribution of southward freshwater transport across Davis Strait. The freshwater transport is widespread from March till May when the region is ice covered, and then it weakens overall from June to August when the flow speed is weak (see Section 3). From September to November, we observe a very large transport in the top western

part of the strait where Tan and Strain (1980) have found most of the meltwater (Fig. 17). This is accompanied by large transports above or on the east side of the ridge, more related to the CIL. Through the winter, the freshwater transport is shifted eastward towards the ridge. It seems that there is a shift from the meltwater influence to the CIL influence. The CIL is closer to the surface at the ridge due to the isopycnal slope. One has to keep in mind that the large freshwater transports are observed above 150 m where we had to make strong assumptions about the salinity. More adequate sampling of the top 150 m will be necessary to confirm these results.

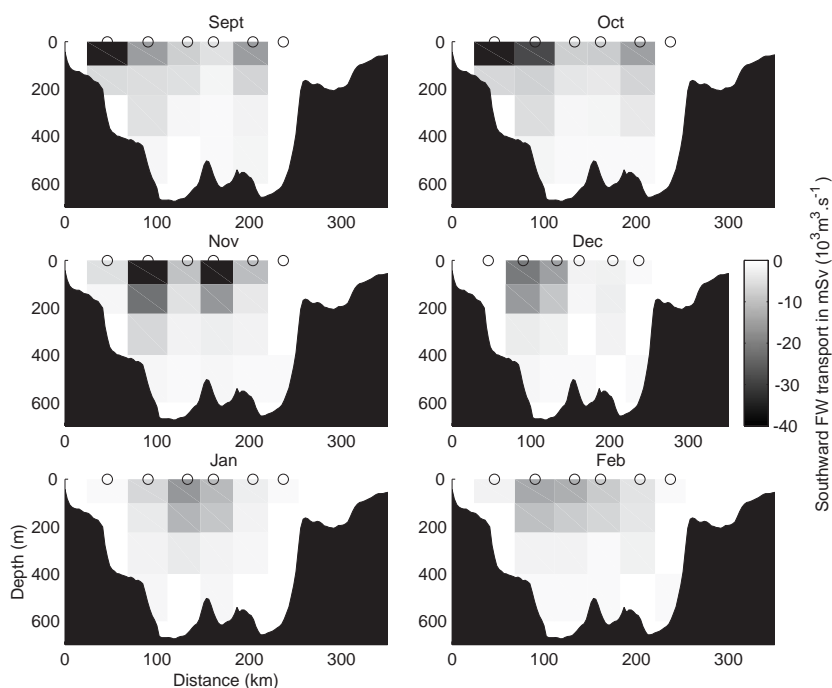


Fig. 17. Southward freshwater transport per bin ( $\text{mSv} = 10^3 \text{ m}^3 \text{ s}^{-1}$ ) deduced from the mooring array for the period September–February. Each bin has approximately the same area which allows for useful comparisons (see text for details). The circles at the surface indicate the mooring locations.

#### 4.3. Sea-ice transport

The sea-ice transport is another component of the freshwater fluxes through Davis Strait. Davis Strait is ice covered at least 6 months of the year (Deser et al., 2002). Sea-ice constitutes a freshwater reservoir under solid form as the ice mostly melts on the Labrador shelf. Using SMMR-SSM/I data, we were able to compute the sea-ice area flux through Davis Strait. We considered a thickness of 0.5 m in December and 1 m from January till May (National Ice center data (<http://www.natice.noaa.gov/eastarct.htm>)) to compute volume fluxes (Fig. 18). Taking into consideration the monthly ice concentration, the mean annual cumulative sea-ice volume flux through Davis Strait over December–May from the 1992–2000 data are  $496 \pm 50 \text{ km}^3$  (Fig. 18b). If we consider the numbers deduced earlier from the work of Jordan and Neu (1982), we can add an additional  $17 \text{ km}^3$  for the sea-ice transport in June–July

(thickness = 0.7 m) and  $15 \text{ km}^3$  in November (thickness = 0.5 m). This gives a total of southward transport of  $528 \text{ km}^3$ .

There is little interannual variability and the correlation between the sea-ice volume transport and the NAO is very weak ( $r = -0.05$ ). This suggests that the larger ice extent in the Labrador Sea in years of high NAO index (Deser et al., 2002) is due to local formation more than stronger southward advection. The correlation between the winter–spring mean meridional winds and the yearly transport is better ( $r = -0.47$ , not significant at 95%, though) (Fig. 18b and d). The correlation between the mean winter–spring meridional winds and the NAO index is close to zero. Using only the meridional winds from December to March or using wind speed instead of meridional wind barely improves the correlation. The NAO index does not appear as a good climatic proxy for the Davis Strait region when the index and the main winds are so little related. There is a

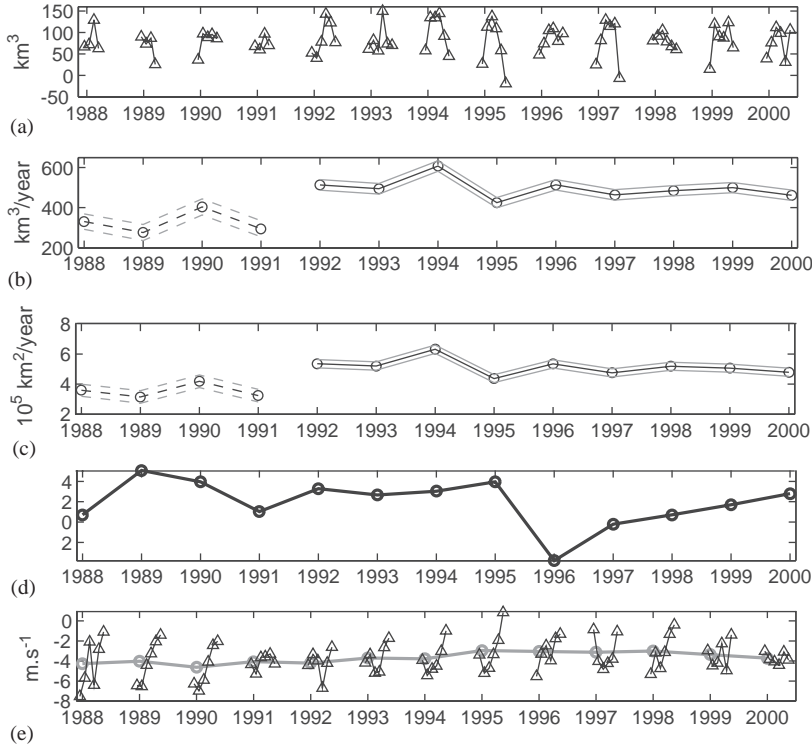


Fig. 18. (a) Monthly mean sea-ice transport ( $\text{km}^3$ ) through Davis Strait for winter spring 1988 through 2000. (b) Yearly cumulative sea-ice volume transport ( $\text{km}^3$ ) through Davis Strait. The corresponding error estimates are represented by the surrounding grey lines. The results for 1988–1991 are drawn with dashed curves because they are not considered as reliable as the results after 1992. (c) Same as for (b) but for the sea-ice area transport in ( $10^5 \text{ km}^2$ ). (d) Winter NAO index. (e) Monthly mean meridional wind ( $\text{m s}^{-1}$ ) for winter spring 1988 through 2000. The winter–spring mean wind speed is given by the thick line with circles. The first marker for each year corresponds to December.

significant variability from month to month with the largest sea-ice transport observed in February–March. The correlation between the monthly transport and the local meridional wind is good during 1992–2000 ( $r = -0.62$ , significant at 95%) but not significant over 1988–1991. We cannot be sure if the weaker correlation is real or just due to the poor quality of the transport estimates before 1992.

In order to obtain fresh water transport equivalent from the sea-ice area flux, we apply the following formula:

$$T_{\text{FWeq}} = \frac{(S_0 - S)}{S_0} \times F_{\text{ice}} \times h \times \frac{C_{\text{ice}}}{100} \times \frac{\rho_{\text{ice}}}{\rho_{\text{water}}}, \quad (2)$$

where  $F_{\text{ice}}$  is the sea-ice area flux ( $\text{km}^2$ ),  $h$  the ice thickness (m),  $C_{\text{ice}}$  the mean sea-ice concentration

across Davis Strait (%),  $\rho_{\text{ice}}$  the sea-ice density ( $900 \text{ kg m}^{-3}$ ) and  $\rho_{\text{water}}$  the density of water ( $1000 \text{ kg m}^{-3}$ ). In this case,  $S_0 = 34.8$  and we assume the sea-ice salinity to be 5. Hence the annual mean transport of  $528 \text{ km}^3$  is equivalent to  $12.9 \text{ mSv}$  of fresh water, which is an order of magnitude smaller than the transport under liquid form.

#### 4.4. Heat transport

We can also compute the heat transport anomaly with respect to  $0^\circ\text{C}$  through Davis Strait using the mooring meridional velocity and the temperature data. We use  $0^\circ\text{C}$  as a reference temperature to allow for comparison with the heat fluxes through more southern latitude lines. The

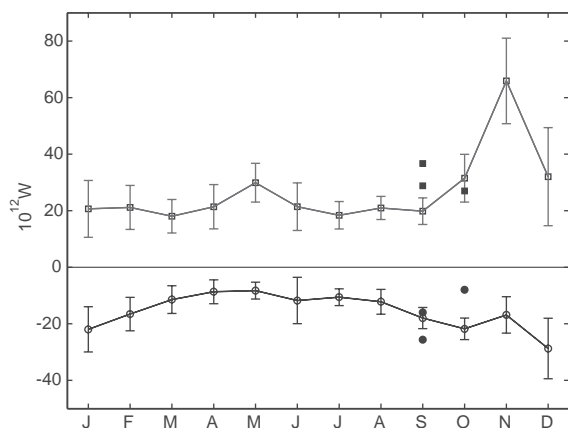


Fig. 19. Monthly mean heat transport (in  $TW = 10^{12} W$ ) through Davis Strait deduced from the 1 year average mooring data, West Greenland shelf excluded. The negative and positive time series are respectively for the southward and northward heat transport. The error bars are the monthly standard deviation. Solid circles and squares represent, respectively, the southward and northward CTD heat transport estimates (see Table 3).

annual mean heat transport anomaly, West Greenland shelf excluded, is  $27 \pm 15 \times 10^{12} W$  northward and  $-15.5 \pm 8 \times 10^{12} W$  southward (Fig. 19). The northward heat transport anomaly is maximum in November and minimum in March, while the southward transport is maximum in December and minimum in April–May.

The northward heat transport anomaly seasonal cycle is influenced by the southward transport in the CIL (with weakly varying sub-zero temperature) (Fig. 10), the ISW and WGS transport and temperature seasonal cycle (see Section 4.1 and Fig. 9).

From hydrographic data, we observe that the southward heat transport anomaly in September 1987 is due to the western surface flow and to a large portion of ISW which gets entrained southward close to the eastern flank of the ridge (Fig. 12c). In October 1988 (Fig. 12f), the western surface flow has already cooled off and is now included in the northward heat transport, while the southward entrainment of ISW has stopped.

Again, we compare the mooring estimates to the CTD estimates to get a more realistic range of uncertainty (Table 3). The average uncertainty is

48% of the mooring estimate for the northward transport and 38% for the southward transport. For the northward heat transport anomaly, the average uncertainty in the top 150 m is as large as for the transport below 150 m. For the southward transport anomaly, the average uncertainty in the top 150 m is half of the uncertainty below 150 m. The CTD heat transport anomaly estimates indicate that on average 50% of the southward heat transport and 50% of the northward heat transport are contained in the top 150 m.

In order to compute the net heat transport through Davis Strait, we have to estimate the annual mean heat transport anomaly on the West Greenland shelf. For this purpose, we used the mooring M6 top instrument combined with historical temperature data. The September and October estimates are  $9.8 \times 10^{12}$  and  $18.8 \times 10^{12} W$  (Table 4). We obtain an annual mean heat transport anomaly of  $6.5 \pm 7.2 \times 10^{12} W$  northward on the shelf. This gives a net heat transport of  $18 \pm 17 \times 10^{12} W$  through Davis Strait, WGS included. Hence the heat transport through Davis Strait represents only 3% of the total estimated northward heat transport into the North Atlantic subpolar gyre ( $0.6 \times 10^{15} W$ ; Ganachaud and Wunsch (2000)).

## 5. Summary and discussion

Using an extensive dataset collected in 1987–1990, we described the circulation in Davis Strait and computed transports. The ridge in the middle of the strait was found to affect the circulation particularly during the spring–summer when the transport is the weakest. We also observed an interesting reversal of the flow at 150 m at M1 from November to February (Fig. 8a, d). This northward flow can reach  $12 \text{ cm s}^{-1}$ . This phenomenon is concentrated in the upper layer of the western portion of the strait as the reversal is not observed at the 300 m instrument at mooring M1 (Fig. 8a, d), nor at mooring M2. The reversal is not due to the bottom topography because it would affect the entire water column, and the arrival of fresher water does not match the current reversal suggesting that this is not a different water mass

suddenly coming from the south (Fig. 10). The density distribution deduced from the mooring array in January (not shown) suggests that upwelling takes place in the western part of the strait. If this upwelling is related to an eastward Ekman transport, it has to be due to a northward stress. This stress could be due to the speed difference between the ocean and the sea-ice which is almost land-fast close to Baffin Island (H. Stern, personal communication). However, the stress could only cancel the velocity but not reverse the flow.

The similarity of the annual cycles in volume and freshwater transport suggest that the Baffin Island Current and the West Greenland Current are predominantly buoyancy driven. The amplitude of the southward freshwater transport annual cycle is more dictated by the flow of meteoric waters coming from Lancaster Sound than by the sea-ice melting-freezing cycle in Baffin Bay. The seasonality in the transport of these two freshwater sources affected the Baffin Island Current structure, with the meltwater flow closer to the coast being stronger in the fall while the CIL flow was stronger in the winter and flowed closer to the middle of the strait. The sea-ice transport through Davis Strait presents significant monthly variability, related to the meridional local wind, but very little interannual variability. We also showed from the heat transport anomaly estimates, that the southward flow of sub-zero CIL is as important as the northward flow of ISW for the northward heat transport anomaly.

Davis Strait plays a fundamental role in the North Atlantic as a connection between the Arctic and the subpolar gyre linking Baffin Bay with the Labrador Sea. Baffin Bay plays a buffer role between the Canadian Archipelago and the Labrador Sea as it is 100% covered with ice in the winter and ice free at the end of summer. The cumulated southward transport through the three main straits of the Canadian Archipelago is about 1–2 Sv (Fissel et al., 1988; Rudels, 1986). The liquid freshwater transport through the archipelago is of the order of 30–40 mSv (Rudels, 1986; Aagaard and Carmack, 1989; Steele et al., 1996). The volume transport compares well with our 2.6 Sv net transport estimate, but the freshwater

estimate is less than half of our estimate of 92 mSv. The earlier estimate is not necessarily unrealistic if we consider the influence of interannual variability and the range of uncertainty associated with our estimate. The discrepancy might also be due to the Canadian Archipelago lack of data, which have led the freshwater transports estimates to be computed by considering an average transport and an average salinity. As a simple test, we estimated the freshwater transport in the western part of the Davis Strait by two different methods: the first one is similar to our earlier calculation where we combined each bin velocity and salinity, and the second consists in multiplying the transport by the mean salinity in the area of interest. Using the 1988 section, which showed only southward flow in the western part of the strait (Fig. 4d), we find that the average value multiplication method gives a result 46% smaller.

The sea-ice transport is assumed negligible through the Canadian Archipelago because the sea-ice is mostly land-fast, whereas it is very large through Fram Strait (annual mean: 64 mSv of FW with a salinity of 5, 2366 km<sup>3</sup>/year in volume (Kwok and Rothrock, 1999)). Hence, the sea-ice transport at Davis Strait (528 km<sup>3</sup>/year) represents slightly more than a fifth of the Fram Strait transport. Meredith et al. (2001) suggest that the liquid southward freshwater transport by the East Greenland Current is two times larger than the equivalent transport by sea ice. From Aagaard and Carmack (1989), we deduce a 5 mSv freshwater transport southward by the saline West Spitsbergen current. Hence the net freshwater transport (liquid + solid) through Fram Strait (197 mSv) is larger than the transport through Davis Strait (105 mSv).

We can try to close the Arctic volume budget as Davis Strait is a more constrained gate to the Arctic than the Canadian Archipelago. We assume that the main passages to the Arctic are the Bering Strait, Fram Strait, Barents Sea, Hudson Strait and Davis Strait. The following values are found in the literature for the volume transports:  $0.8 \pm 0.3$  Sv for Bering Strait (Roach et al., 1995),  $-1.7 \pm 2.0$  Sv for Fram Strait (Fahrbach et al., 2001),  $1.6 \pm 1.2$  Sv for the Barents Sea (Mauritzen, 1996) and  $-0.1 \pm 0.3$  Sv for Hudson

Strait (Drinkwater, 1988). The river runoff contributes around 0.1 Sv. This leaves net transport of 0.7 Sv for the Canadian Archipelago-Davis Strait exit. This is smaller than our estimate of 2.6 Sv.

Using the estimates collected by Carmack (2000), we try the same exercise for the freshwater transports. The total arctic runoff including mainland and arctic islands is  $4269 \text{ km}^3 \text{ yr}^{-1}$  (135.3 mSv, Vuglinsky (1997)). Bering Strait liquid freshwater inflow is  $1670 \text{ km}^3 \text{ yr}^{-1}$  (52.9 mSv, Aagaard and Carmack (1989)). Small amount of ice coming through Bering Strait constitutes  $24 \text{ km}^3 \text{ yr}^{-1}$  (0.7 mSv, Aagaard and Carmack (1989)). Precipitation minus evaporation represents  $1944 \text{ km}^3 \text{ yr}^{-1}$  (61.6 mSv) as obtained from NCEP and ECMWF (Bromwich et al., 2000). The Norwegian Coastal Current through Barents Sea represents  $330 \text{ km}^3 \text{ yr}^{-1}$  (10.4 mSv). The salty flow through the Barents Sea provides a negative contribution to the freshwater budget of  $-540 \text{ km}^3 \text{ yr}^{-1}$  (-17.1 mSv, Aagaard and Carmack (1989)). We have mentioned earlier a net freshwater transport of  $-6235 \text{ km}^3 \text{ yr}^{-1}$  (-197 mSv) through Fram Strait. There is no good freshwater flux estimate for Hudson Strait, so we will use the lower end of the range suggested by Mertz et al. (1993):  $946 \text{ km}^3 \text{ yr}^{-1}$  or 30 mSv.

This leads to a net of  $516 \text{ km}^3 \text{ yr}^{-1}$ , i.e. 16.3 mSv of fresh water, which is close to the lower end of our estimate range for Davis Strait. The inter-annual variability being so large at all the sources, a simultaneous monitoring within the same pentade would clearly help to refine the Arctic Ocean budget.

## Acknowledgements

The authors would like to thank Charlie Ross from BIO for collecting and providing the Davis Strait dataset analyzed in this manuscript. Suggestions from several people at BIO (Brian Petrie, Charles Tang and Igor Yashayaev) and from three reviewers were helpful for improving the manuscript. Finally, we would like to thank Luanne Thompson and Craig Lee for their thorough editing of a first version of the manuscript.

## References

- Aagaard, K., Carmack, E.C., 1989. The role of sea ice and other fresh water in the Arctic circulation. *Journal of Geophysics Research* 94 (C10), 14485–14498.
- Agnew, T., Le, H., Hirose, T., 1998. Estimation of large scale sea ice motion from SSM/I 85.5 GHz imagery. *Journal of Geophysics Research* 25 (Ann. Glaciol.), 305–311.
- Bacon, S., Reverdin, G., Rigor, I., Snaith, H., 2002. A freshwater jet on the east Greenland shelf. *Journal of Geophysics Research* 107 (C7) 5–1–5–16.
- Bromwich, D., Cullather, R., Serreze, M., 2000. Reanalyses depictions of the Arctic moisture budget. In: Lewis, E. (Ed.), *The Freshwater Budget of the Arctic Ocean*. NATO Science series. Kluwer Academic Publishers, Dordrecht (Chapter 8).
- Carmack, E., 2000. The Arctic Ocean's freshwater budget: sources storage and export. In: Lewis, E. (Ed.), *The Freshwater Budget of the Arctic Ocean*. NATO Science series. Kluwer Academic Publishers, Dordrecht (Chapter 5).
- Chapman, D., Beardsley, R., 1989. On the origin of shelf water in the Middle Atlantic Bight. *Journal of Physical Oceanography* 19, 384–391.
- Cuny, J., Rhines, P.B., Niiler, P.P., Bacon, S., 2002. Labrador Sea boundary currents and the fate of the Irminger Sea Water. *Journal of Physical Oceanography* 32 (2), 627–647.
- Deser, C., Holand, M., Reverdin, G., Timlin, M.S., 2002. Decadal variations in Labrador Sea Ice Cover and North Atlantic Sea surface temperatures. *Journal of Geophysics Research* 107.
- Drinkwater, K., 1988. On the mean and tidal currents in Hudson Strait. *Atmosphere Ocean* 26, 252–266.
- Fahrbach, E., Meincke, J., Osterhus, S., Rohardt, G., Schauer, U., Tverberg, V., Verduin, J., 2001. Direct measurements of volume transports through Fram Strait. *Polar Research* 20 (2), 217–224.
- Fissel, D., Birch, J., Melling, H., Lake, R., 1988. Non-tidal flows in the North-West Passage. Canadian technical report of hydrography and ocean sciences 98, Fisheries and Ocean Canada.
- Ganachaud, A., Wunsch, C., 2000. Improved estimates of global ocean circulation, heat transport and mixing from hydrographic data. *Nature* 408, 453–457.
- Goosse, H., Fichefet, T., Campin, J.-M., 1997. The effects of the water flow through the Canadian Archipelago in a global ice-ocean model. *Geophysics Research Letters* 24 (12), 1507–1510.
- Hamilton, J., Prinsenberg, S., Malloch, L., 2002. Moored current meter and CTD observations from Barrow Strait 1998–1999. Canadian data report of hydrography and Ocean Sciences 157, Fisheries and Ocean Canada.
- Houghton, R., Visbeck, M., 2002. Quasi-decadal salinity fluctuations in the Labrador Sea. *Journal of Physical Oceanography*, 687–701.
- Ingram, R., Prinsenberg, S., 1998. Coastal oceanography of Hudson Bay and surrounding eastern Canadian Arctic waters. In: Robinson, A., Brink, K. (Eds.), *The Sea*, vol. 11. Wiley, New York, pp. 835–861.

- Jones, E.P., Swift, J., Anderson, L., Lipizer, M., Civitarese, G., Falkner, K., Kattner, G., McLaughlin, F., 2003. Tracing Pacific water in the North Atlantic Ocean. *Journal of Geophysics Research* 108, 13 1–13 10.
- Jordan, F., Neu, H., 1982. Ice drift in southern Baffin Bay and Davis Strait. *Atmospheric Ocean* 20 (3), 268–275.
- Khatiwala, S., Schlosser, P., Visbeck, M., 2002. Rates and mechanisms of water mass transformation in the Labrador Sea as inferred from tracer observations. *Journal of Physical Oceanography*, 666–686.
- Kwok, R., Rothrock, D.A., 1999. Variability of Fram Strait ice flux and North Atlantic Oscillation. *Journal of Geophysics Research* 104 (C3), 5177–5189.
- Kwok, R., Schweiger, A., Rothrock, D.A., Pang, S., Kottmeier, C., 1998. Sea ice motion from satellite passive microwave data assessed with ERS and buoy motion. *Journal of Geophysics Research* 103, 8191–8214.
- Lazier, J.R.N., Wright, D.G., 1993. Annual velocity variations in the Labrador Current. *Journal of Physical Oceanography* 23 (4), 659–678.
- Lemon, D., Fissel, D., 1982. Seasonal variations in currents and water properties in northwestern Baffin Bay, 1978–1979. *Arctic* 35 (1), 211–218.
- Liu, A., Cavalieri, D., 1998. On sea-ice drift from wavelet analysis of Defense Meteorological Satellite Program (DMSP) special sensor microwave imager (SSM/I) data. *International Journal of Remote Sensing* 19, 1415–1423.
- Loder, J.W., Petrie, B., Gawarkiewicz, G., 1998. The coastal ocean off North-Eastern North America: a large-scale view. In: Robinson, A.R., Brink, K.H. (Eds.), *The Sea*, vol. 11. Wiley, New York, pp. 105–133.
- Macdonald, R.W., Carmack, E.C., McLaughlin, F.A., Iseki, K., Macdonald, D., O'Brien, M., 1989. Composition and modification of water masses in the Mackenzie shelf estuary. *Journal of Geophysics Research* 94 (C12), 18057–18070.
- Mauritzen, C., 1996. Production of dense overflow waters feeding the North Atlantic across the Greenland-Scotland ridge. Part 2: an inverse model. *Deep-Sea Research I* 43, 807–835.
- Melling, H., Gratton, Y., Ingram, G., 2001. Ocean circulation within the North water Polynya of Baffin Bay. *Atmosphere-Ocean* 39 (3), 301–325.
- Meredith, M., Heywood, K., Dennis, P., Goldson, L., White, R., Fahrbach, E., Schauer, U., Østerhus, S., 2001. Freshwater fluxes through Fram Strait. *Geophysics Research Letters* 28 (8), 1615–1618.
- Mertz, G., Narayanan, S., Helbig, J., 1993. The freshwater transport of the Labrador Current. *Atmosphere-Ocean* 31 (2), 281–295.
- Myers, R., Akenhead, S., Drinkwater, K., 1990. The influence of Hudson Bay runoff and ice-melt on the salinity of the inner Newfoundland shelf. *Atmosphere-Ocean* 28 (2), 241–256.
- Roach, A., Aagaard, K., Pease, C., Salo, S., Weingartner, T., Pavlov, V., Kulakov, M., 1995. Direct measurements of transport and water properties through the Bering Strait. *Journal of Geophysics Research* 100, 18443–18457.
- Ross, C., 1990a. Currents and temperature data from north-western Baffin Bay, september 1983–1984. Canadian data report of hydrography and ocean sciences 78, Fisheries and Oceans Canada.
- Ross, C., 1990b. Currents and temperature data from south-western Baffin Bay, October 1984–1985. Canadian data report of hydrography and ocean sciences 79, Fisheries and Oceans Canada.
- Ross, C., 1992. Moored current meter measurements across Davis Strait. NAFO Research Document 92/70.
- Rudels, B., 1986. The outflow of polar water through the Arctic Archipelago and the oceanographic conditions in Baffin Bay. *Polar Research* 4, 161–180.
- Shiklomanov, I., Shiklomanov, A., Lammers, R., Peterson, B., Vorosmarty, C., 2000. The dynamics of river water inflow to the arctic ocean. In: Lewis, E. (Ed.), *The Freshwater Budget of the Arctic Ocean*. NATO Science series. Kluwer Academic Publishers, Dordrecht (Chapter 13).
- Steele, M., Thomas, D., Rothrock, D., Martin, S., 1996. A simple model study of the Arctic Ocean freshwater balance, 1979–1985. *Journal of Geophysics Research* 101 (C9), 20 833–20 848.
- Tan, F., Strain, P., 1980. The distribution of sea ice meltwater in the eastern Canadian Arctic. *Journal of Geophysics Research* 85 (C4), 1925–1932.
- Vuglinsky, V., 1997. River inflow to the arctic ocean: conditions of formation time variability and forecasts. In: *Polar Processes and Global Climate*. ACSYS, pp. 275–276.
- Wadley, M.R., Bigg, G.R., 2002. Impact of flow through the Canadian Archipelago and Bering Strait on the North Atlantic and Arctic Circulation: an ocean modelling study. *Quarterly Journal of the Royal Meteorological Society* 128 (585), 2187–2203.